ACS OMEGA

http://pubs.acs.org/journal/acsodf

Article

Screening the Degradation of Polymer Microparticles on a Chip

Seyed Mohammad Davachi, Amir Mokhtare, Hooman Torabi, Mojtaba Enayati, Ted Deisenroth, Toan Van Pho, Liangliang Qu, Katrin-Stephanie Tücking, and Alireza Abbaspourrad*

Cite This: *ACS Omega* 2023, 8, 1710−1722

Read Online

ACCESS | Metrics & More | Article Recommendations | Supporting Information

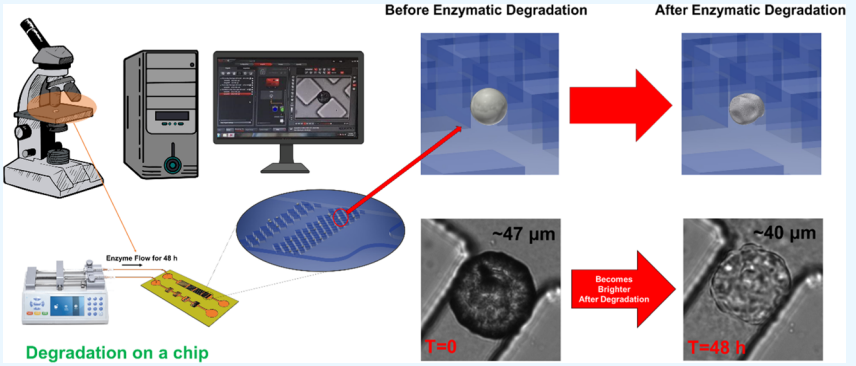

ABSTRACT: Enzymatic degradation of polymers has advantages over standard degradation methods, such as soil burial and weathering, which are time-consuming and cannot provide time-resolved observations. We have developed a microfluidic device to study the degradation of single microparticles. The enzymatic degradation of poly (1,4-butylene adipate-*co*-terephthalate) (PBAT) microparticles was studied using Novozym 51032 cutinase. PBAT microparticles were prepared via an oil-in-water emulsion solvent removal method, and their morphology and chemical composition were characterized. Then, microparticles with varying diameters of 30−60 μm were loaded into the microfluidic chip. Enzyme solutions at different concentrations were introduced to the device, and changes in the size and transparency of PBAT microparticles were observed over time. The physicochemical properties of degraded products were analyzed by FT-IR, NMR, mass spectrometry, and differential scanning calorimetry. The degradation process was also performed in bulk, and the results were compared to those of the microfluidic method. Our analysis confirms that the degradation process in both bulk and microfluidic methods was similar. In both cases, degradation takes place on aliphatic and soft segments of PBAT. Our findings serve as a proof of concept for a microfluidic method for easy and time-resolved degradation analysis, with degradation results comparable to those of conventional bulk methods.

INTRODUCTION

Petroleum-based plastics are highly utilized materials, with a production rate of 380 million tons per year (2015).[1] However, the limitations of petroleum resources, environmental concerns associated with using such materials, and legislative pressure[2] motivated researchers to develop environmentally friendly substitutions, which resulted in the introduction of biodegradable polyesters in the 1980s.[3]

Aromatic polyesters, such as polyethylene terephthalate, satisfy the physicochemical properties required for several applications, but they are well known for their lower biodegradability rates compared with aliphatic polyesters.[2] Alternatively, aliphatic polyesters, such as polylactic acid and polyhydroxy butyrate, suffer from high rigidity and low elongation at break, which limits their applications.[1] To address these issues, poly (1,4-butylene adipate-*co*-terephthalate) (PBAT) was developed by BASF. PBAT is a linear random co-polyester of 1,4 butanediol and adipic acid dimers (BA) that serve as flexible (soft) units, along with crystalline terephthalic acid and 1,4 butanediol dimers (BT) that serve as rigid (hard) units.[4,5] The copolymerization of BA and BT units provides biodegradability, flexibility, longer elongation at break, hydrophilicity, and better processability.[6] PBAT is considered a fully compostable polyester according to ASTM D6400,[7] and its microbial degradation has been extensively studied.[3] Furthermore, PBAT hydrolysis and degradation by erosion have been reported[4,8] and it has been confirmed that the aliphatic region in PBAT is the most susceptible to degradation. In addition, anaerobic sludge changes the crystallinity of PBAT during degradation.[9] Although field test methods such as soil burial and composting, simulate

Received: December 2, 2022
Accepted: December 14, 2022
Published: December 23, 2022

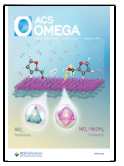

environmental degradation conditions, they are time-consuming and have a limited scope of analysis. For instance, soil burial biodegradation and composting tests are validated after 180 days and 24 months, according to ISO 17088 and ASTM D5988, respectively.[10] All the contributing factors in the simulated degradation environments are well defined.[11] In addition to environmental conditions, the degradation rate of polymers depends on their physicochemical and morphological properties.[12,13] PBAT is not water soluble and therefore has low bioavailability. As a first step, microorganisms must secrete extracellular enzymes to catalytically hydrolyze the ester bonds to provide water-soluble intermediates. Once the polymers are broken down into smaller, water-soluble intermediates, microorganisms take up these intermediates and further metabolize them to CO_2 to complete the degradation cycle. The enzymatic hydrolysis step is considered the rate-controlling step in biodegradation[11] and, as a result, the enzymatic degradation of biodegradable polymers has been the subject of numerous studies. Enzymatic degradation of polyesters by lipase was first reported in 1977.[14] Since then, several studies have focused on finding various types of enzymes isolated from different microorganisms, which can perform polyester degradations.[2,3,11,15−19] To broaden the application of biodegradable polyesters, especially for cargo release purposes and biomedical applications, a time-resolved degradation profile in a predefined environment is required. Current degradation analysis for bulk samples is time-consuming, often requiring multiple tests of similar samples at different time intervals, which makes them unable to provide real-time measurements.[20,21] Also, evaluation of the extent of degradation in bulk samples requires offline analysis of degraded samples, making these methods time- and resource-demanding. Real-time analytical methods, such as quartz crystal microbalance, surface plasmon resonance, and scanning photoinduced impedance microscopy, have been previously utilized to decrease the time and increase throughput when studying the polymer degradation process.[22] However, these methods are expensive, require special apparatus, and offer limited analysis of different polymer morphologies.

A microfluidic system is an inexpensive method that can be used as a platform for the real-time degradation analysis of polymers with different morphologies. Interestingly, very few studies in this field have been reported using these platforms. Integrated microfluidic devices with capacitive field effect sensors to monitor the real-time degradation of polymers[20−22] and the use of microfluidic devices in the study of flow-induced degradation have been reported.[23] Furthermore, it was found that degradation of polymeric nanoparticles on enzyme-immobilized microchannels integrated with liquid chromatography was faster than bulk degradation analysis.[24] Pulsatile release of pharmaceuticals has been the subject of several studies for its advantages over other drug administration methods. In this regard, the manufacturing of microfluidic chips with the pulsatile release of nucleic acids and other therapeutics triggered by the degradation of a thin film has been reported.[25,26] However, to the best of our knowledge, the visualization of enzymatic degradation of polymeric microparticles in microfluidic devices has not been investigated. Microparticles have a higher surface area relative to mass (higher aspect ratio) compared with macroparticles. Considering that enzymatic degradation takes place on the surface of the substrate, we observe that polymer degradation is substantially accelerated as the particle size decreases and the aspect ratio increases. The accelerated degradation can help us make faster assessments on the degradation behavior.[12]

We have found a facile method for real-time visualizations of enzymatic degradation of polymeric microparticles using microfluidic devices: degradation on a chip (DOC). We observed that upon degradation, PBAT undergoes a change in size and transparency, which is related to the extent of degradation. Furthermore, the regions of the PBAT that contain terephthalates are more robust to enzymatic degradation, so as particles lose mass, they become transparent. The flow of the chip, however, is gentle enough that they are not crushed and retain their shape. This proof of concept provides information supporting the possibility of using this method over conventional degradation techniques, providing fast and real-time observations in a high-throughput fashion to find the optimal conditions for bulk polymer degradation.

2. MATERIALS AND METHODS

2.1. Materials. PBAT was generously provided by BASF. Novozym 51032 (15 KLU/g) was acquired from Strem Chemicals Inc. (MA, USA). Polyvinyl alcohol (PVA, Mowiol 10−98, $M_w \sim 61000$ g/mol), 1,4-butanediol (Bd, ReagentPlus ≥ 99%), adipic acid (Ada, ≥99.5%, BioXtra, HPLC grade), formic acid (ACS reagent, Ph. Eur., ≥98%), methanol (HPLC, ≥99.9%), hydrochloric acid (HCl, ACS Reagent, 37%), chloroform (HPLC, ≥99.8%), Tween 80, and sodium chloride (NaCl, ACS Reagent ≥99%) were all purchased from Sigma-Aldrich (St. Louis, USA). Tris(hydroxymethyl)aminomethane (Tris, ACS Reagent) was obtained from Chem-Impex Int'l (IL, USA). Terephthalic acid (Ta, 99+ %) was bought from Acros Organics. Phosphate buffer saline (PBS) 100 mL tablets were bought from Research Products International (IL, USA). Rhodamine B (RhB, HY-Y0016) and Nile red (NR, HY-D0718) were purchased from MedChemExpress (NJ, USA). In all the steps, ultrapure water was used, which was purified using a Milli-Q (MQ) integral water purification system, Merck Millipore Corp., (Darmstadt, Germany).

2.2. Particle Preparation. The microparticles were prepared using the oil-in-water solvent evaporation method with some modifications.[27−29] It has been reported that a change in the concentration of the emulsifier (PVA) can affect the size of the microparticles.[28,30] To prepare microparticles in the desired range of 40−70 μm, the concentration of PVA in the mixture must first be optimized. For this purpose, 100 mL of PVA solutions in MQ water at different concentrations (2.5, 3.5, 4, and 5 w/v %) was prepared. The organic phase was prepared by dissolving 5 g of PBAT in 50 mL of chloroform (10% w/v). Then, the organic phase was added to the flask containing the PVA solution and mixed using a mechanical stirrer (IKA Eurostar 40 digital, Germany). The mixture was stirred at 500 rpm for 15 min at room temperature, warmed to 45 °C, and held there for 5−6 h until all the chloroform evaporated. The produced microparticles from each concentration of PVA solution were assessed for their particle size range using an optical microscope. As shown in Table 1, 4 w/v % PVA solution showed the desired particle size, while the increase and decrease in PVA concentration produced microparticles with smaller and larger sizes, respectively. Two nylon mesh filters were used to collect the microparticles. A 60 μm filter (U-CMN-60, Component Supply Co., Tennessee, USA) was used to collect the larger microparticles on the filter. The filtrate was then passed through a 38 μm (U-CMN-38) nylon mesh filter that collected the desired sized microparticles

https://doi.org/10.1021/acsomega.2c07704
ACS Omega 2023, 8, 1710−1722

Table 1. Particle Sizes of PBAT Samples at Different Concentrations of PVA

no	PVA concentration (w/v %)	particle size (μm)
1	2.5	50−120
2	3.5	30−80
3	4	40−70
4	5	10−56

on the filter for use in the microfluidic chip. The microparticles between 38 and 60 μm were collected on the filter, washed with MQ water, freeze-dried using a Labconco FreeZone 1 (USA) at 0.074 mbar and −50 °C for 24 h, and stored under ambient conditions.

2.3. Microfluidic Device Fabrication and Operation. Standard planar soft lithography techniques were used to fabricate the polydimethylsiloxane (PDMS) microfluidic devices.[31,32] The micropatterned PDMS layer has a main channel consisting of square cross-section pillars, whose surface density increases from the inlet port toward the outlet port. The schematic and photographs of the final device are shown in Figure 1A−D. The more precise dimensions of the designed chip are depicted in Figure S1. To obtain the final devices, we designed a series of chips, as shown in Figure S2. In the final design, because of the pillars, we can visualize the real-time degradation of a single particle in a specific location.

Device operation involves three consecutive steps. First, we washed the microfluidic device with a dilute Tween 80/MQ water solution (0.25 w/v %) to minimize surface absorption and inadvertent clogging. Second, we inject the microparticles suspended in a density-matched NaCl solution (33 w/v %) to prevent their agglomeration. To prevent clogging, the sample solution should be sparse; therefore, 4 mg/mL of microparticles in MQ water solution were prepared, and Tween 80 (0.25 w/v %) was used to assist with the suspension of the microparticles. The solution was vigorously mixed on a vortex shaker and then injected into the chip. The injection of the sample is visually assessed until a sufficient number of microparticles for the experiment are trapped in the field of view of the microscope (Figure S2). After loading the particles to ensure that the emulsifier was removed completely, we

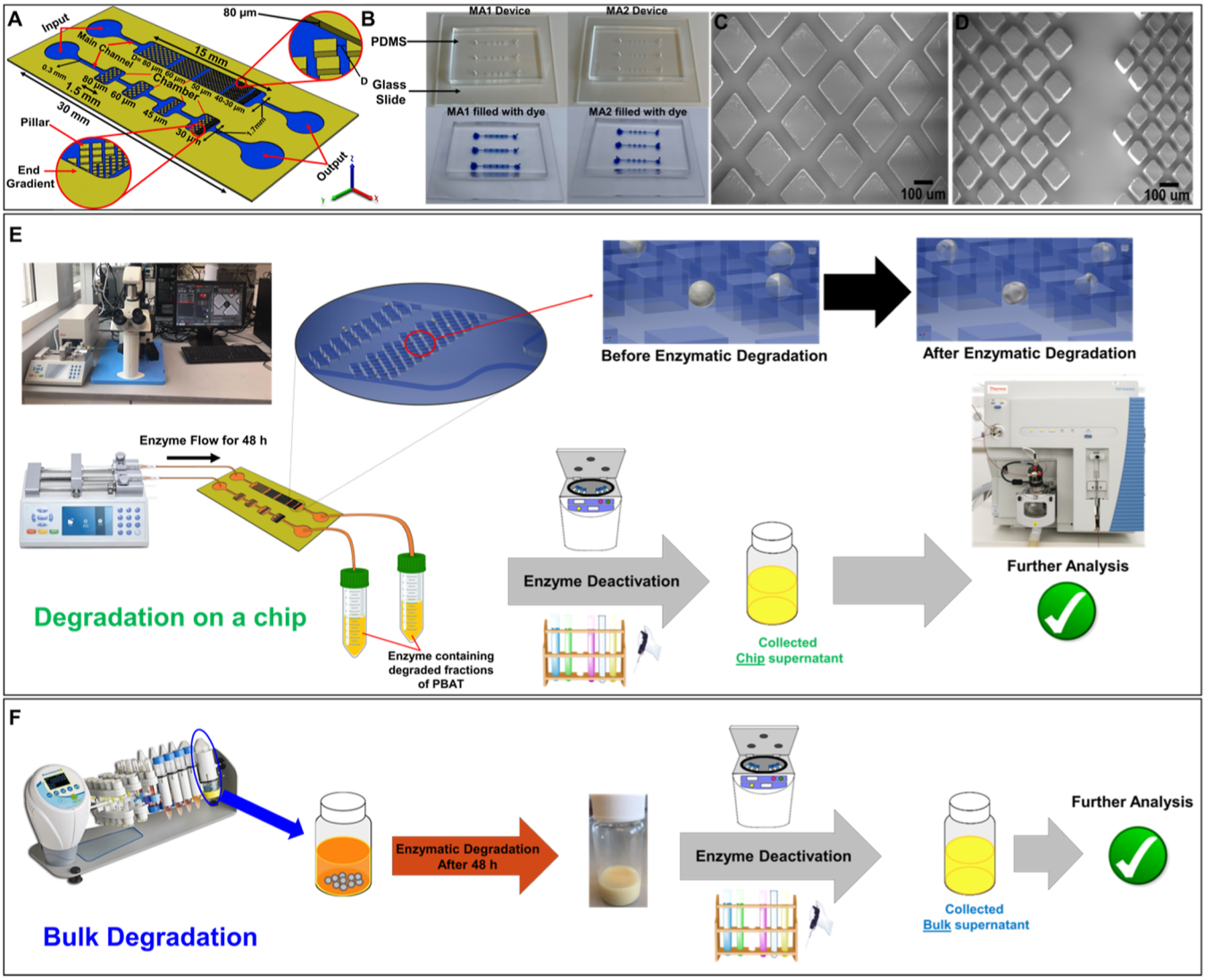

Figure 1. (A) Schematic presentation of the microfluidic chip designs for observation of degradation on a chip. (B) Photograph images of microfluidic devices before and after filling with blue dye. SEM images of (C) the chip chamber and the pillar (D) gradient in the pillared chips. Schematic of enzymatic degradation in the (E) chip and (F) bulk (agitated with a programmable rotator).

https://doi.org/10.1021/acsomega.2c07704
ACS Omega 2023, 8, 1710−1722

washed the channels and microparticles with 3−4 mL MQ water for 15 min. The estimated pore volume of the chips is ∼2 to 2.5 μL. The position of the device was fixed on the microscope stage and fresh enzymatic solution was injected to start the degradation process for 48 h with injection speeds, depending on the experiment, between 25 and 100 μL/h, and the solution was collected for further steps. In addition, for microscopic studies, time-lapse images were taken at 15 min intervals over 48 h.

2.4. Bulk Enzymatic Degradation of Microparticles. To compare the microfluidic chip results with conventional methods, we also assessed the direct enzymatic degradation of PBAT microparticles, which we will call the bulk method. In this method, the microparticles will be directly exposed to the enzyme. The bulk microparticle samples were obtained by adding specific amounts of microparticles into 5 mL of enzyme solution with various concentrations for 48 h.

2.5. Enzyme Deactivation Procedure. To examine the results of polymer degradation, the enzyme was deactivated and removed by methanol precipitation from the collected solution from the chip or the bulk samples. To deactivate and remove the enzymes, after 48 h, the samples from the bulk and the chip were collected, and ice-cold methanol was added to the sample and controls with a 1:1 ratio (v/v). The samples were put in ice for 10 min, then transferred to falcon tubes and placed into the centrifuge chamber at 0 °C for an additional 10 min without spinning. After incubation, the samples were centrifuged (Thermo Scientific, Heraeus Multifuge X1R Centrifuge, USA) for 15 min at 0 °C with 22,000*g*. The supernatant is collected and acidified using HCl to reach a pH of 3.0, and the acidified solution was then incubated in a fridge (4 °C) for 2 h. The solid is collected separately and acidified using the same conditions, then washed with MQ water 3−4 times, centrifuged for 10 min at 7000*g*, and freeze-dried. The acidified supernatant was put in a centrifuge chamber and incubated for 10 min at 0 °C and subsequently centrifuged (15 min, 0 °C, 22,000*g*).[2,3,33] The supernatant is again collected, and to increase the solubility of the degradation products, the pH was adjusted to 8.5 using 50 mM Tris buffer. The collected supernatant and freeze-dried solid parts were both used for further analysis. The schematic of the degradation on the chip and in the bulk can be seen in Figure 1E,F.

2.6. Characterization. *2.6.1. Fourier-Transform Infrared-Attenuated Total Reflection Spectroscopy (FTIR-ATR).* IRAffinity-1S FTIR, equipped with a Quest single reflection ATR module (Specac, Kent, UK), was used to obtain the IR spectra of the PBAT microparticles before and after enzymatic degradation. The test was performed at a resolution of 4 cm^{-1} (averaging 128 scans) and in the frequency range of 400−4000 cm^{-1}.

2.6.2. Thermal Properties. Differential scanning calorimetry (DSC) was performed using Q2000 TA Instruments (New Castle, DE, USA) according to ASTM D3418. The DSC tests were performed in the temperature range of −60 to 270 °C under a N_2 atmosphere and at a heating rate of 10 °C/min.

2.6.3. Nuclear Magnetic Resonance. ^{1}H NMR (500 MHz) and ^{13}C NMR (125 MHz) spectra were recorded using the Bruker Avance-500 spectrometer at 30 °C. $CDCl_3$ and DMSO-d_6 were used as the solvent for PBAT before and after degradation, respectively.

2.6.4. Thin Layer Chromatography. For an initial assessment of the presence of degradation products, thin layer chromatography was used. Briefly, 2 μL of the reaction mixture was applied to boron-impregnated silica gel G-25 plates (layer thickness of 0.25 mm). The plate was immersed in a mobile phase consisting of methanol/ethyl acetate (50:50 v/v) so that the mobile phase covered up to 3 mm of the lower edge of the plate. Then, the plate was air-dried for 15 min at room temperature. The images are exposed at 254 nm, and the plates were analyzed by comparing the mobility of the products from the chip and bulk samples with known compounds.

2.6.5. Mass Spectrometry. The supernatant was analyzed for degradation products using liquid chromatography with tandem mass spectrometry (LC−MS). Samples were injected into an Agilent 1100 HPLC coupled to a Finnigan LTQ mass spectrometer with an ESI ion source (Thermo Electron Corporation, Germany). The solution of 60% MQ water and 40% methanol with 0.1% formic acid at a flow rate of 0.4 mL per min was used as a mobile phase. The HPLC column used was Luna 3 μm C18 non-polar and was kept at an ambient temperature. The injection volume was 5 μL, and the injections were repeated three times for each sample. Same ion source parameters were used for positive and negative ion modes. Auxiliary and sheath gas flow rates adjusted at 15 and 50 au, respectively. The spray, capillary, and tube lens voltages were set at 4.0 kV, 41.0 V, and 125 V, respectively. Finally, the capillary temperature was set at 350 °C. The samples were initially run in the first stage of mass spectrometry (parent mass, MS^1) in a normal scan range and resolution settings (50−1000 m/z) to verify the presence of monomers and degraded products. Then, to determine the best transition ions, the selective reaction monitoring (SRM) analysis of the potential degradation product in the second stage of mass spectrometry (MS^2) was carried out.[2] The total run time for all samples and scan types was 45 min.

To confirm the LC−MS results, the collected bulk supernatant and enzyme solution passed through the chip and collected after degradation were also analyzed with SYNAPT-G2Si-high-definition mass spectrometry quadrupole time-of-flight (HDMS Q-TOF) fitted with an atmospheric solid analysis probe (ASAP) ion source (Waters Corp, Manchester, United Kingdom). The test was done by the mass spectrometry laboratory at the University of Illinois Urbana-Champaign with optimal parameters as follows: capillary voltage of 3 kV and cone voltage at 25 V. The gas sheath and cone flow were maintained at 500 and 60 L/h, respectively. The ASAP probe temperature was progressed from 100 to 500 °C. The scan time and inter-scan delay were set to 0.3 and 0.1 s, respectively. A full scan mode was used for MS collection from m/z 50 to 1000.

We used the enzyme solution as received, and the presence of ∼32% propanediol and other unidentified additives in the enzyme solution caused variations in LC−MS results, especially with respect to butanediol release. Therefore, for any experiments that were analyzed using LC−MS, the enzyme was purified via ultrafiltration (Amicon Ultra-50 Centrifugal Filter Unit, Ultracel, 10 kDa, 50 mL, MilliporeSigma, USA) as reported elsewhere.[2,34]

2.6.6. Microscopic Observations. Initial assessment of the particle size and degradation process in the chip was observed under a Leica Model DMIL LED Inverted Phase Contrast (IPC) Microscope at 10/20×. The mean diameters of average 50 microparticles in each sample were analyzed using ImageJ software (v1.53a, NIH, USA).

To observe the particle sizes and degradation products in the bulk and chip methods, scanning electron microscopy (SEM)

https://doi.org/10.1021/acsomega.2c07704
ACS Omega 2023, 8, 1710−1722

(Zeiss Gemini 500 Field Emission, Germany) was used at an accelerating voltage of 1.0 kV. The SEM samples were coated with a 15 nm layer of Au−Pd via the Denton Desk V sputter coater (Moorestown, NJ, USA) before the test.

2.6.7. Confocal Laser Scanning Microscopy. The porous structure and the degradation of the PBAT microparticles on a chip were examined using a confocal laser scanning microscope (CLSM, Carl Zeiss LSM 880, Göttingen, Germany), with the help of the z-stack method. For observation of the porous structure, Nile red (NR) was added (2 w/v %) to the chloroform during the initial preparation of the microparticles. For observation of degradation on a chip, 2 w/v % solution of rhodamine B (RhB) in MQ water was mixed with the microparticles after their preparation.[35] For the chip, the prepared solution of RhB was injected into the chip, and the microparticles were stained with RhB for 24 h. Then, Milli-Q water was injected to wash the excess dyes with continuous washing for 24 h. In all the staining procedures, to ensure that the fluorescent color (NR and RhB) does not degrade by the light, the whole setup was kept in the dark. The stained microparticles were visualized using excitation/emission wavelengths of 492/518 nm for NR and 510/568 nm for RhB, respectively.

2.7. Statistical Analysis. Analyses were performed by one-way analysis of variance (ANOVA), followed by Tukey's multiple comparisons in triplicates using Origin software (Version 9, MA, USA), and the results were presented as mean ± standard deviations.

3. RESULTS AND DISCUSSION

To investigate the effect of the enzyme on the degradation of the PBAT, the microparticles were initially assessed before and after enzymatic degradation in bulk (15 mg/5 mL).

3.1. Characterization of Microparticles. *3.1.1. FTIR Spectra.* The FTIR-ATR spectra of the neat PBAT and enzymatically degraded PBAT in bulk are shown in Figure 2. The neat PBAT and PBAT microparticles had similar FTIR results; therefore, the neat PBAT was reported as a representative.

The IR spectrum of neat PBAT exhibits bands at 2956 and 2873, which are attributed to the stretching vibrations of CH_2, and 1710 cm^{-1}, which relates to the C═O stretching vibration. The benzene skeleton vibration is observed at 1507 cm^{-1}. The bands at 1409 and 1388 cm^{-1} belong to the trans-CH_2−plane bending vibration. The band at 1267 cm^{-1} is related to the symmetric stretching vibration of C−O, while the peak at 1104 cm^{-1} belongs to the left-right symmetric stretching vibration of C−O. The bending vibration of the phenyl ring's contiguous hydrogen atoms can be observed at 1016 cm^{-1}. Finally, the absorptions at 935 and 727 cm^{-1} represent the trans-C−O symmetric stretching vibration and CH-plane of the benzene ring, respectively.[6] After enzymatic degradation, the absorptions were either shifted or the intensities decreased. The enzymatically degraded PBAT shows the lower intensity bands of stretching vibrations of CH_2 at 2945 and 2866 cm^{-1}, while the C═O stretching vibration bands are also shifted to 1681 cm^{-1}. The absorptions at 1278 and 1101 cm^{-1}, which belong to the stretching vibrations of C−O and 1423 cm^{-1} related to the CH_2 bending vibration, show drastically lower intensity and are also shifted when compared to the neat PBAT. The bands at 1507, 935, and 727 cm^{-1}, which all belong to the benzene ring, have only shown a decrease in their intensities, which is evidence that the enzyme was not able to degrade them as much as the linear sections of PBAT.

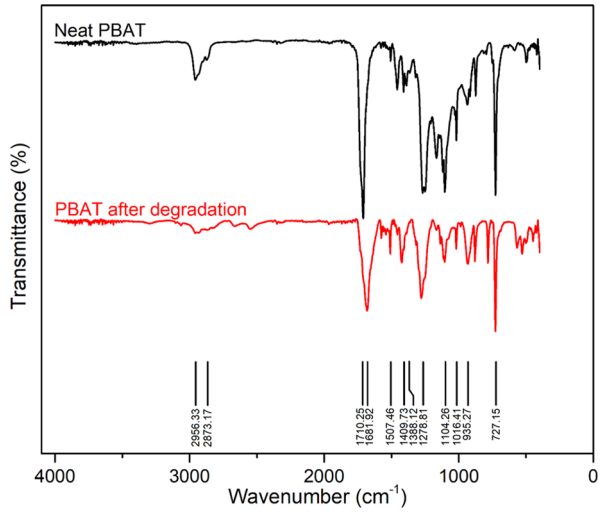

Figure 2. FTIR spectra of PBAT before and after degradation in bulk.

3.1.2. Differential Scanning Calorimetry Analysis. The crystallization behavior and thermal properties of the PBAT before and after degradation were observed by differential scanning calorimetry (DSC), and the results reported in Table 2. The glass transition temperature (T_g) of the neat granules and microparticles of PBAT are nearly the same, while upon enzymatic degradation, the T_g shows a remarkable increase. The melting temperature (T_m), melting enthalpy (ΔH_m), and crystallinity (X_c) all decreased in the PBAT microparticles compared with the neat PBAT; this was a result of using organic solvents for the preparation of the microparticles, which disturbed the conformation of the sample. After enzymatic degradation, the remaining PBAT showed an increase in the T_m, ΔH_m, and X_c compared to the neat PBAT, which is a good indicator of degradation. PBAT consists of hard butylene terephthalate (BT) and soft butylene adipate (BA) segments. These soft and hard segments have close cohesive energy with a relatively similar chain conformation and a crystal lattice, which allows the soft segments to fit into the hard segments to establish a co-crystallization or mixed crystallization structures.[7] Therefore, the soft BA segment, which is mainly amorphous, is less compact and is more susceptible to enzymatic degradation. After degradation, mostly BT units remain because they are less susceptible to enzyme degradation, and thus, due to their inherent higher crystallinity, T_m increases.[4] The increase in ΔH_m and X_c in the enzymatically degraded microparticles of

Table 2. Thermal Properties of PBAT Before and After Degradation

samples	T_g (°C)	T_m (°C)	ΔH_m (J/g)	X_c[a] (%)
PBAT	−35.51	120.79	12.82	10.75
PBAT microparticles	−35.45	110.32	6.41	5.62
enzymatically degraded PBAT microparticles	27.28	159.09	22.81	20.01

[a]Considering the melting enthalpy of 100% crystalline PBAT 114 J/g.[7]

https://doi.org/10.1021/acsomega.2c07704
ACS Omega 2023, 8, 1710−1722

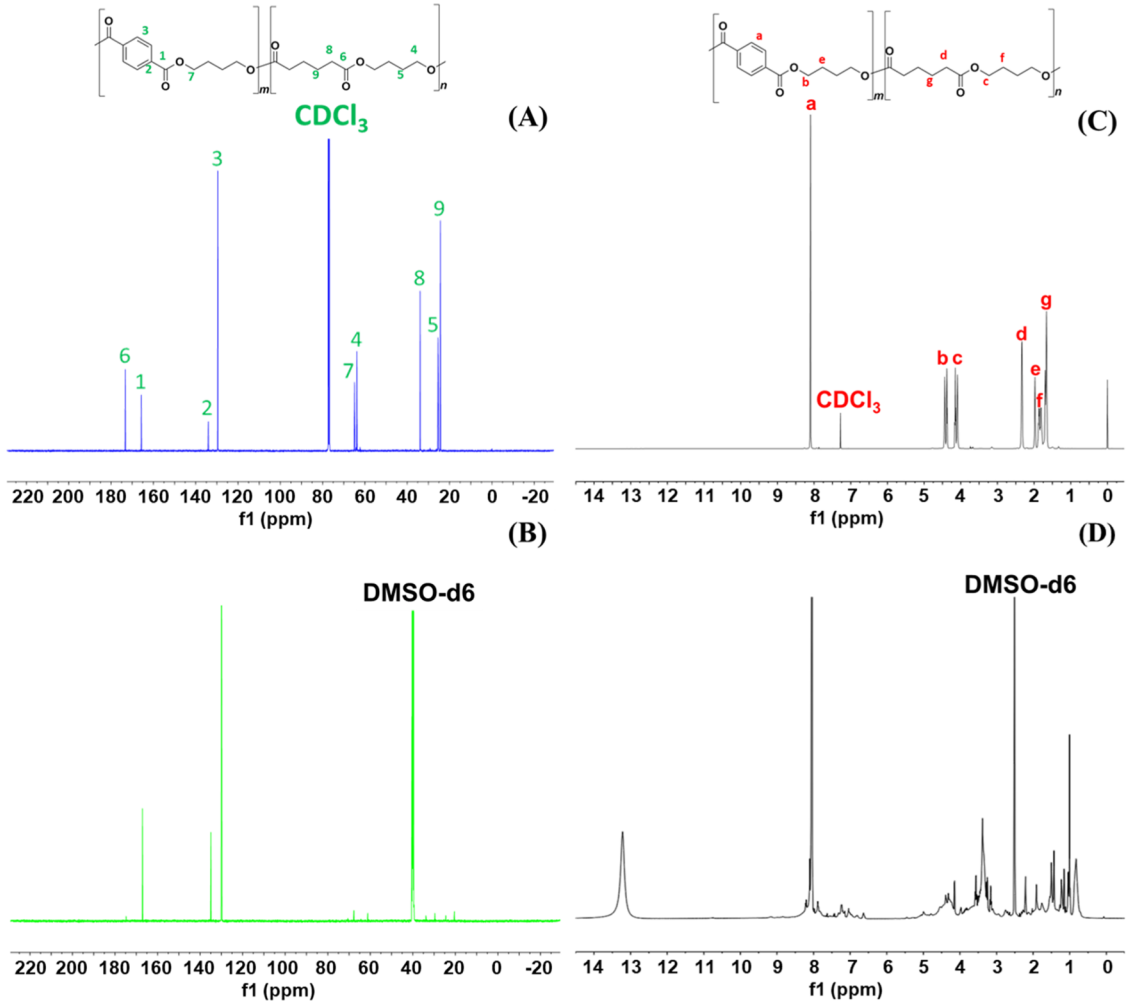

Figure 3. ^{13}C NMR (125 MHz) of pure PBAT (A) and (B) after 48 h of enzymatic degradation. The ^{1}H NMR (500 MHz) spectra of pure PBAT (C) and (D) after 48 h of enzymatic degradation.

PBAT means that the amorphous regions have been degraded by the enzyme, while the hard segment units with more terephthalate structures remain undegraded. The T_g of PBAT is negative, and the polymer has a rubber-like consistency; however, after degradation, the PBAT has a firm, chalky consistency, which is further evidence of intact terephthalates.

3.1.3. NMR Studies. The chemical structure of the PBAT before and after degradation was characterized using ^{13}C NMR and ^{1}H NMR spectra (Figure 3). The ^{13}C NMR of the neat PBAT shows two signals at 173.2 ppm (6) and 165.7 ppm (1) assigned to the carbonyl groups of the BA and BT units, respectively. The aromatic carbons of the BT unit are observed at 134.0 ppm (2) and 129.5 ppm (3). The signal at 63.8 ppm (7) belongs to the inner CH_2 in butanediol of the BT unit. Finally, the peaks at 64.8 ppm (4) and 25.3 ppm (5) are related to the inner CH_2 in butanediol of the BA unit, while the peaks at 33.8 ppm (8) and 24.3 ppm (9) are attributed to the inner CH_2 groups in adipic acid in the BA unit.[36] Supporting the observations found in the FTIR and DSC analyses in the enzymatically degraded PBAT, only the terephthalate signals are observable since the aliphatic units have been fully degraded. Because the degraded products did not dissolve in $CDCl_3$, DMSO-d_6 was used as the solvent.

The ^{1}H NMR spectra of neat PBAT show the peak of the CH group of the benzene ring in the BT unit at 8.10 ppm (a), while the butanediol outer and inner CH_2 groups of the BT segment can be detected at 4.37−4.44 ppm (b) and 1.66 ppm (e). The signals at 2.33 ppm (d) and 1.67−1.69 ppm (g) belong to the outer and inner CH_2 groups of adipic acid in the BA unit. In addition, the butanediol outer and inner CH_2 groups of the BA segment can be observed at 4.10−4.15 ppm (c) and 1.69 ppm (h). Butanediol shows another inner CH_2 group signal at 1.79−1.90 ppm (f) in the BA segment.[36] The adipate to terephthalate ratio was obtained to be 50:50 using ^{1}H NMR (Figure S3), and our results are in accordance with previous reports.[2]

The enzymatically degraded PBAT NMR results show only the presence of terephthalic acid and terephthalates after the degradation, which explains the difference in solubility and confirms our observations in the thermal and vibrational data. The PBAT soft segment (BA) has degraded, and the major components left are the hard segments; thus, the particle becomes less dense, more transparent, and yet retains its shape because of the gentle nature of treatment.

3.1.4. Microscopic Studies of the Microparticles. To observe the size of the microparticles for use in the microfluidic chip, we initially used an IPC microscope. The microparticles prepared with a 4 w/v % PVA stabilizer show a spherical shape and smooth surface with a size between 38 and 70 μm (Figure 4A). Even after filtration, some small

https://doi.org/10.1021/acsomega.2c07704
ACS Omega 2023, 8, 1710−1722

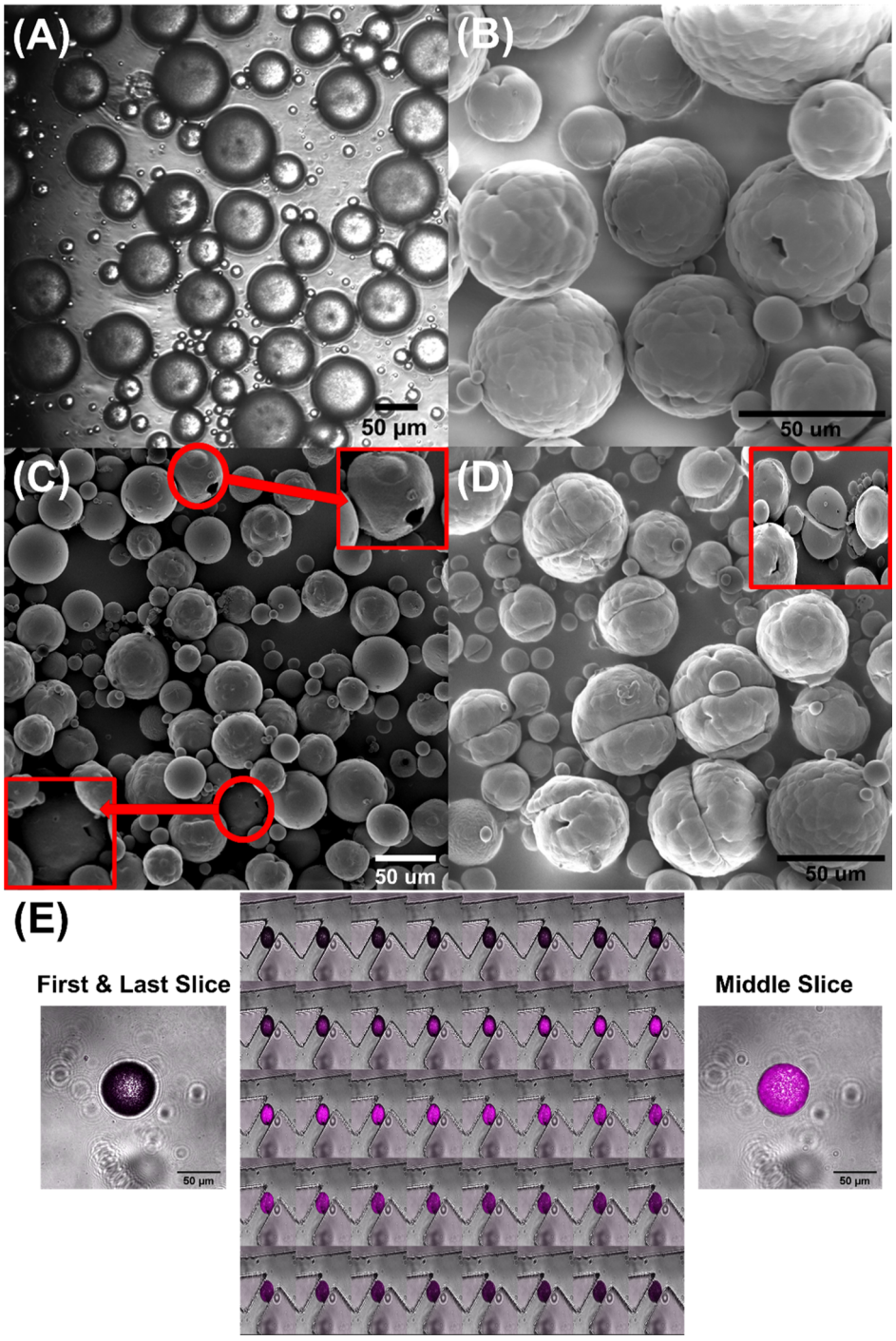

Figure 4. (A) IPC microscopy image of PBAT microparticles with 4 w/v % PVA. SEM of PBAT microparticles; (B) porous structure; (C) core–shell structure (inset is a close up of the shell), holes indicate that the inside of the particle is hollow; (D) solid structure showing lines from blade cuts (inset shows a close up of the interior revealed by the cut); and (E) CLSM z-stack pictures of PBAT stained with Nile red.

microparticles remain; however, this amount would not block the chip and is flushed from the system after initial injection. The structure of the prepared microparticles was also assessed by SEM, and the microparticles show a pitted, potentially more porous structure on the surface (Figure 4B). There are some particles that have big holes, which increases the possibility that there may be some hollow structures as well (Figure 4C). To further confirm the inside structure of the microparticles, we sliced the microparticles using a new, sharp blade and found that they are mostly solid microparticles with a porous surface (Figure 4D).

To confirm the porous structure of the inside of the microparticles, Nile red (NR) was added to the chloroform during the initial preparation of the microparticles, and the microparticles were stained. The prepared microparticles were assessed with CLSM, and the porous structure can be confirmed in Figure 4E, middle, first, and last slices; the surface is not colored, while the middle slice shows the highest intensity of NR color. Since only the core has been stained and

https://doi.org/10.1021/acsomega.2c07704
ACS Omega 2023, 8, 1710−1722

the NR color is hydrophobic,[37] we postulated that the surface is hydrophilic. During microparticle preparation, the hydrophobic (hard) segments of PBAT stay in the core, while the shell is made of the hydrophilic (soft) segments.

3.2. LC−MS Results. To quantify the enzymatic degradation after 48 h, we designed three sets of experiments that are shown in Table 3. In the first set, we compared the different weights of PBAT in constant enzyme concentrations in bulk. In the second experiment, we assessed the effect of enzyme concentration at constant PBAT weight in bulk. Finally, in the third set, we observed the degradation of the small amount of microparticles in the chip and bulk. After each set of experiments, the enzyme was deactivated (mentioned in Section 2.5), and LC−MS was performed. The potential enzymatic degradation products and intermediates of PBAT previously detected using LC−MS showed that we could expect butanediol (Bd), adipic acid (Ada), terephthalic acid (Ta), mono(4-hydroxybutyl) terephthalate (BTa), and bis(4-hydroxybutyl) terephthalate (BTaB)[2] (Figure 5A). The presence of terephthalic acid and other degradation fractions was initially identified qualitatively by thin layer chromatography (Figure S4) and HDMS Q-TOF ASAP (Figure S5) and then quantified by LC−MS.

Table 3. Enzymatically Degraded Samples Obtained from Chip and Bulk with Different PBAT Microparticle Contents and Enzyme Concentrations

samples	PBAT weight (mg)	enzyme volume (mL)	enzyme concentration (KLU/g)	PBS 7.4[c] (%)
S1	150	5	15	
S2	48	5	15	
S3	15	5	15	
S4	10	5	15	
S5	15	5	11	25
S6	15	5	7.5	50
S7	15	5	3.7	75
S8	0.55	1.2	15	
S9 (chip)[a]	∼0.543	1.2[b]	15	

[a]Solution was passed through the chip and collected after degradation. [b]Enzyme was injected into the chip at 25 μL/h for 48 h to provide a total of 1.2 mL. [c]Percentage of PBS 7.4 buffer used to dilute the enzyme solution.

The polymer to enzyme ratio has a direct effect on the release of the degradation products, which are mostly the monomers of the PBAT (Figure 5B). At a fixed enzyme concentration, the addition of 15 mg PBAT in 5 mL of enzyme (S3) caused the degradation products of the soft segment monomers (Ada and Bd) to increase; however, at higher concentrations of PBAT, these monomers decreased. The Ta does not show a significant difference between all the samples ($p < 0.05$), while BTa and BTaB show an increase of up to 48 mg of PBAT and then decrease with increasing PBAT content. Such behavior could be due to the larger surface area and vicinity of the PBAT microparticles at lower concentrations, while at higher PBAT weights, the by-products prevent enzyme activity and hydrolysis efficiency by lowering the pH.[38,39] When 150 mg of PBAT (S4) is used, the lower results are due to the ester bonds being in close proximity to bulky aromatic groups, which are less accessible for hydrolytic cleavage by the enzyme due to steric hindrance.[40] As expected, decreasing the concentration of enzymes decreases degradation products (Figure 5C).

To compare the microfluidic chip versus bulk methods, we used ∼0.55 mg of PBAT with 1.2 mL of enzyme for both kinds of starting materials. The chip samples show slightly higher values of Bd, Ada, and Ta when compared with the bulk samples. We believe that this is due to the precision of the microfluidic chip when compared to the bulk process (Figure 5D). In the static bulk system, the hydrolyzed intermediates and degradation products may inhibit the enzymatic degradation, affecting the kinetics and hydrolysis efficiency. However, in a continuous flow microfluidic chip system, the inhibitory products flow out of the chip and therefore will have less effect on the enzymatic hydrolysis efficiency and associated kinetics. The initial weight of microparticles loaded into the chip was estimated by counting the number of microparticles trapped in each section by size and then using the density of the PBAT (1.25 g/cm^3); the initial weight loaded in the chip is calculated to be ∼540 μg. The difference in the methods, therefore, could be related to the difference in microparticle loading. To prevent such errors, we performed three separate chip experiments to ensure that the observed results are due to the efficiency of the chip.

The results clearly show the efficiency of the chip in quantifying the PBAT degradation. Degradation in this microfluidic device takes place at higher rates when compared to the bulk method due to the continuous flow of the fresh enzyme. Additionally, the possibility of real-time visualization could provide a convenient method to observe physical changes in particles during enzymatic degradation processes.

3.3. Observation of Degradation of PBAT on a Chip Using Microscopic Studies. To observe the degradation of the microparticles on a chip, we injected the microparticles in the pillared chips, and once enough microparticles were trapped, the enzyme buffered at pH 7.4 was injected into the chip at a flow rate of 50 μL/h. Images of the chip with the loaded microparticles at the initial time (Figure 6A1) and after 48 h of enzymatic degradation (Figure 6A2) show that the PBAT microparticles become brighter and more transparent after enzymatic degradation compared to the initial microparticles. We attribute this increased transparency to the increasing porosity of the microparticle from enzyme degradation. As the porosity increases, more water moves through the microparticle, causing the refractive index to approach that of the water, and therefore, particles appear transparent.

To investigate the possible hydrolytic degradation of PBAT particles, we performed a similar experiment on the particles using an enzyme-free phosphate buffer solution at pH 7.4 and a flow rate of 100 μL/h for 48 h (Figure S6), and no change in particle size and transparency was observed, indicating that the degradation of PBAT's backbone does not take place within this time frame and without the presence of the enzyme. Figure 6B shows the enzymatic degradation of a single PBAT microparticle in the chip, with pillars at representative time points (0, 12, 24, and 48 h). The PBAT particle size decreased, the microparticles became corrugated, and the roughness increased after 48 h of enzyme exposure. A single PBAT microparticle particle size was measured using ImageJ software before and after enzymatic degradation was observed (Figure 6C). The starting microparticle size was ∼47 μm, and during degradation, the size decreased to ∼40 μm, a nearly 15% decrease. To further confirm the change in transparency, we

https://doi.org/10.1021/acsomega.2c07704
ACS Omega 2023, 8, 1710−1722

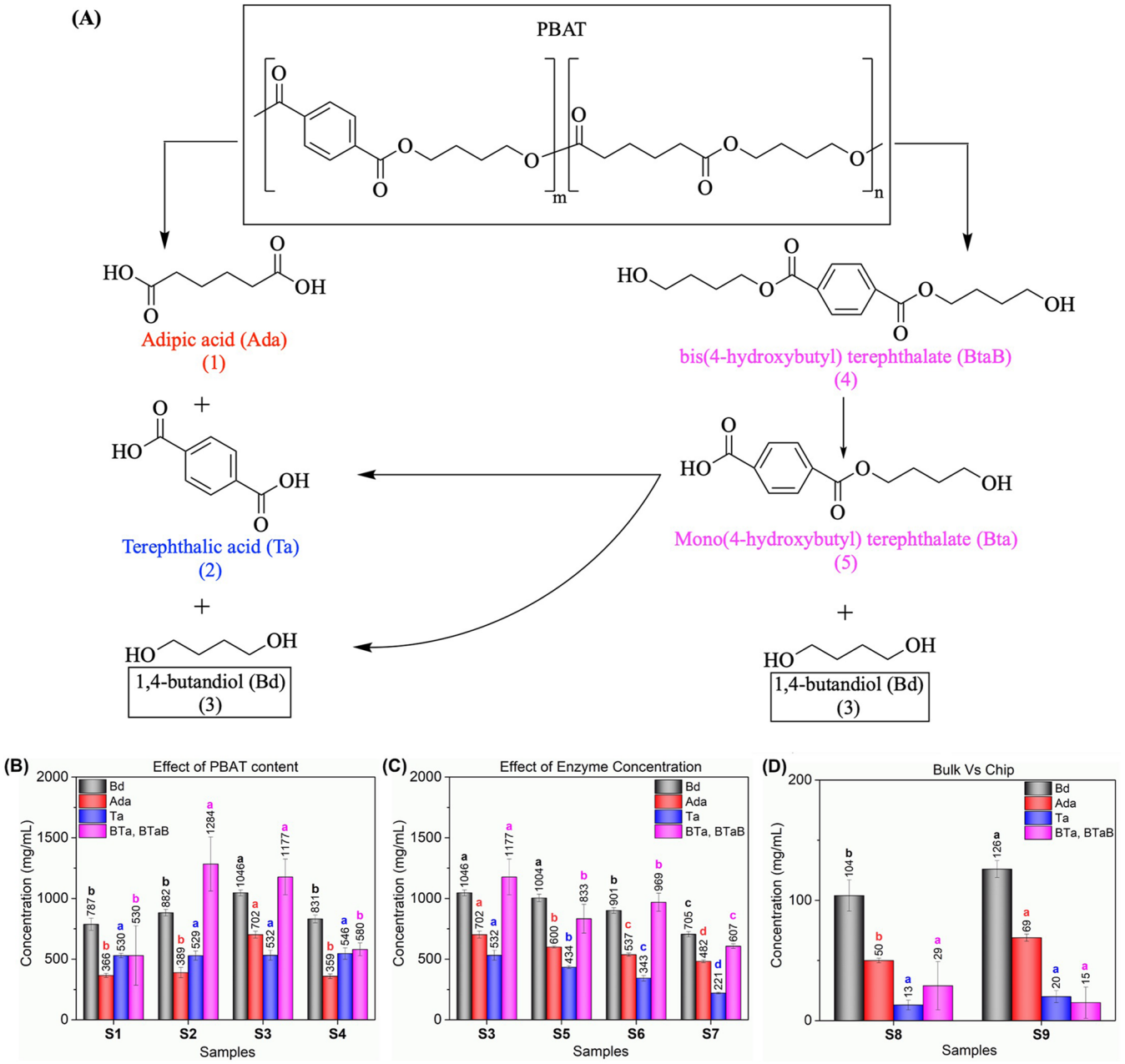

Figure 5. (A) Schematic of potential degraded products after enzymatic degradation. LC−MS results of enzymatic degradation of microparticles for 48 h; (B) effect of PBAT content at bulk; (C) effect of enzyme concentration at bulk; (D) bulk vs chip at a lower enzyme volume. Detailed information of samples S1−S9 is available in Table 3.

took time-lapse pictures of the single microparticles every 15 min (Movie S1) and obtained the transparency values using ImageJ software (Figure 6D). The obtained curves demonstrate an initial darkening and then an increase in the transparency values after 48 h. The darkening in the microparticles could be due to either the surface adsorption of the enzyme and the change in the refractive index of the microparticles or increased light scattering under brightfield conditions, or a combination of both.

To evaluate the effect of enzyme concentration on PBAT degradation we diluted the enzyme and plotted the transparency versus time (Figure 6E). The results show that the enzyme concentration has a direct effect on the speed of polymer degradation. Furthermore, a lower concentration shows wider and longer initial darkening, and the maximum of the transparency values or brightness change at a lower concentration of enzyme happens at longer times when compared to the higher concentrations.

We confirmed that our chip can be used with other polymers by also degrading poly ε-caprolactone (PCL) (Figure S7A). Within 70 min, PCL microparticles treated an enzyme concentration of 15 KLU/g (50 μL/h) became both transparent and lost structure. The loss of structure can be attributed to the absence of aromatic regions in PCL. Similar to our work with PBAT, we confirmed using PCL that the enzyme concentration matters (Figure S7B). Lower enzyme concentration exhibits a wider and longer initial darkening, and once the concentration of enzyme decreases, the PCL shows a longer degradation time. Changing the enzyme concentration allowed us to observe the change in transparency for longer

https://doi.org/10.1021/acsomega.2c07704
ACS Omega 2023, 8, 1710−1722

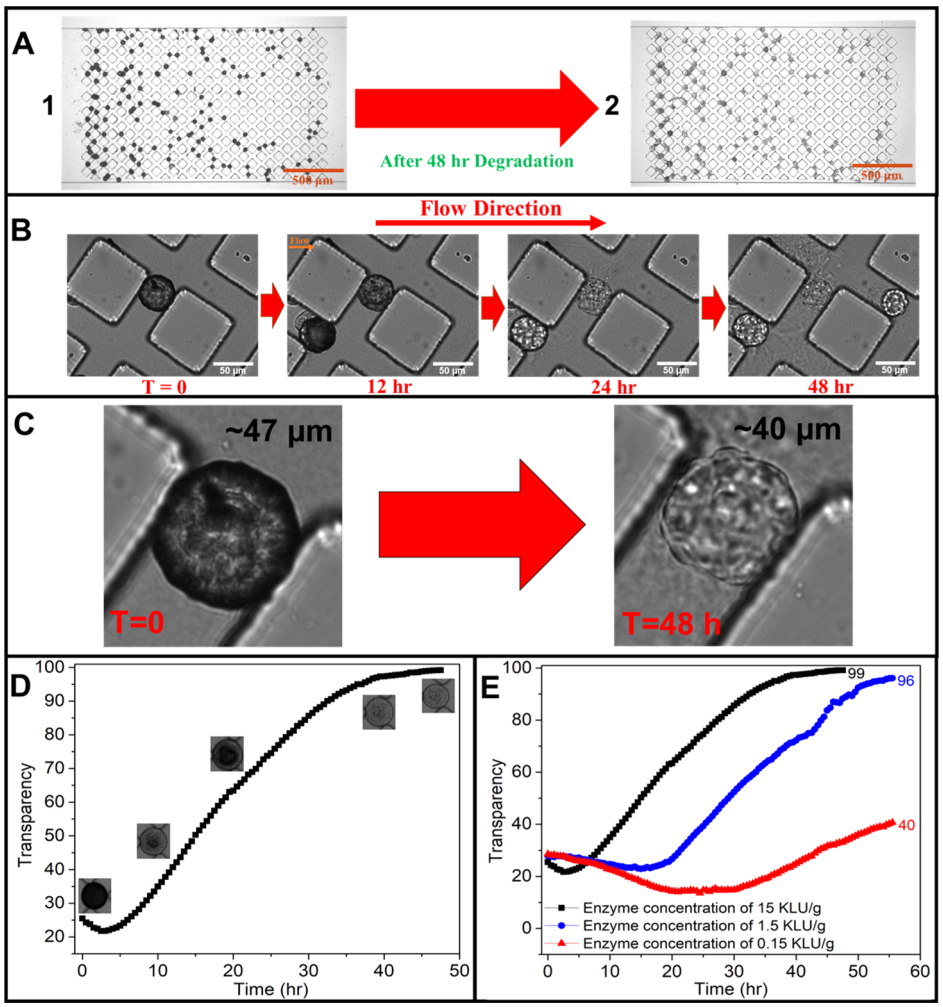

Figure 6. Degradation of the PBAT microparticles in the chip at pH 7.4 and a flow rate of 50 μL/h (A) lower zoom (1) initially and (2) after 48 h of enzymatic degradation. (B) Single particle at different time points; (C) difference in particle size after 48 h; (D) change in transparency values vs time (E) effect of the enzyme concentration on transparency values.

periods of time by visibly slowing down the degradation. This confirms the ability to use this device for enzymatic degradation analysis to observe the impact of using different concentrations of enzyme solutions.

To confirm the degradation results, the CLSM was taken from the RhB-stained particle before and after degradation (Figure S8). The middle slice of the CLSM z-stack is a representative of the other microparticles; noticeably, the surface of the PBAT microparticles was stained by hydrophilic RhB,[37] while the core was either unstained or only showed a slight amount of red color (Figure 7A). This confirmed our observation regarding the hydrophobicity of the core, as indicated by the Nile red stain. However, after enzymatic degradation, the microparticles in both chip and bulk demonstrate the high-intensity red color in the middle slice of the z-stack, indicating that the polymer is degraded or hydrolyzed (Figure 7B,C).

Upon enzymatic degradation, PBAT microparticles maintain their integrity and become more porous. The enzymatic hydrolysis of the PBAT makes it possible for RhB's large aromatic moiety to interact with mostly aromatic degradation leftovers, the terephthalates.[41] Therefore, the color penetrates further inside the degraded structure. The bulk samples are unable to maintain their integrity, possibly due to agitation, and an agglomeration of the degradation leftovers is observed.

The microparticles were assessed using SEM images after 48 h of enzymatic degradation in both bulk and chip. It can be seen in Figure 7D that the degraded products in bulk show a deteriorated and chalky structure as compared to the spherical and slightly smooth PBAT microparticles, which could be due to the shear forces applied to the microparticles during bulk degradation (Figure 4). We were able to retrieve microparticles from the chip after degradation, and as can be observed, the microparticles in the chip maintain their integrity even after degradation (Figure 7E), but their smooth surface is visibly corrugated and rough after 48 h of enzyme exposure.

4. CONCLUSIONS

In the current study, we observed the enzymatic degradation of PBAT on a microfluidic chip. For this purpose, microparticles were prepared using an oil-in-water emulsion, and the microparticles were characterized before and after enzymatic degradation. Microparticles have a higher surface area relative to their mass. Once the size is smaller, the degradation is quicker, and there is more control for optimizing the environmental factors. Furthermore, observing polymer degradation in microparticle samples can provide insights

https://doi.org/10.1021/acsomega.2c07704
ACS Omega 2023, 8, 1710−1722

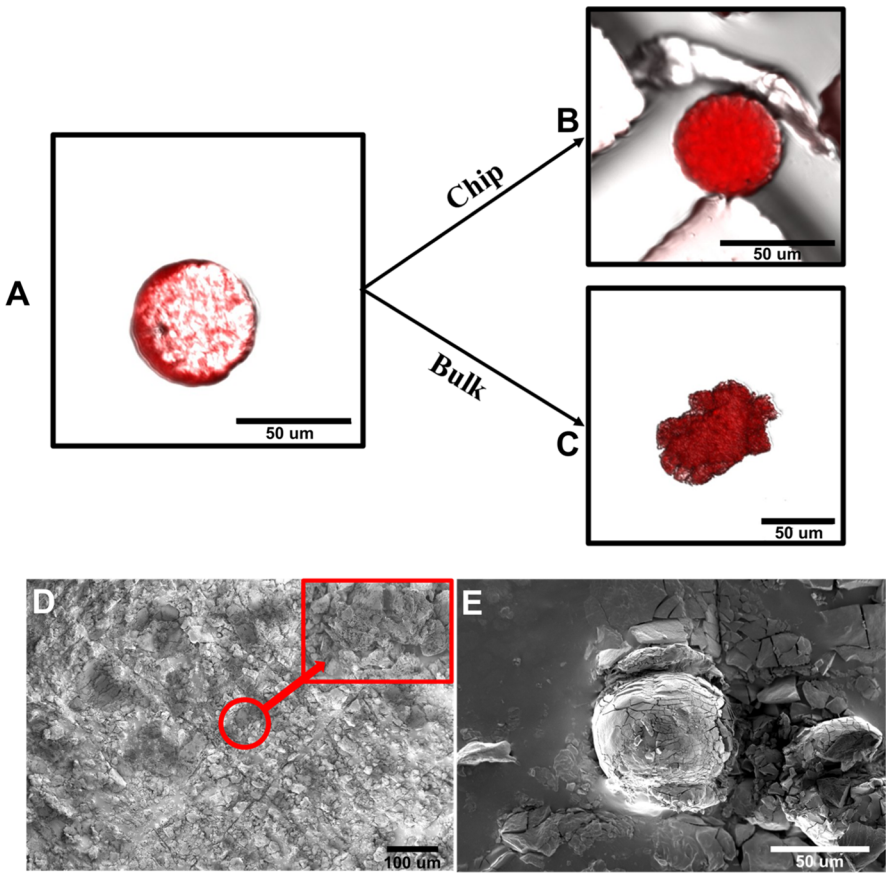

Figure 7. CLSM z-stack middle slice pictures of PBAT microparticles stained with Rhodamine B (A) before and after degradation in the (B) chip and (C) bulk. SEM images of PBAT microparticles after degradation for (D) degraded particles in bulk after agitation in a programable rotator (E) retrieved from the chip.

into the degradation of bulk samples. Therefore, we fabricated a laminar flow design for real-time direct visualization of individual microparticles' enzymatic degradation in a microfluidic chip using microscopy. This efficient and easy method has all the advantages of other bulk methods and offers a continuous flow of the enzyme solution through the chip, which washes the hydrolyzed intermediates and inhibitory products away from the microparticles. As a result, the degradation kinetics and hydrolysis efficiency are not impacted. Additionally, microparticles maintain their integrity after 48 h of degradation, while the degraded microparticles in the bulk disintegrate into smaller pieces due to shear forces during tumbling. DOC enables the visualization and quantification of individual microparticles based on the change in particle diameter and transparency, provides the opportunity to perform replications simultaneously, and reduces the screening time. Our proof-of-concept-designed DOC has been shown to be fast and reproducible, with precise control over temperature, pH, and enzyme concentration.

■ ASSOCIATED CONTENT

Supporting Information

The Supporting Information is available free of charge at https://pubs.acs.org/doi/10.1021/acsomega.2c07704.

Design evolution; ^{1}H NMR of PBAT; thin layer chromatography of reaction mixtures before and after degradation; HDMS Q-TOF ASAP results of reaction mixtures; PBAT degradation on a chip using an enzyme-free phosphate buffer solution at pH 7.4; PCL degradation on a chip using an enzyme solution at pH 7.4 and a flow rate of 50 μL/h and transparency changes versus time during the enzymatic degradation of a PCL at different concentrations; and z-stack stained with Rhodamine B (PDF)

PBAT degradation on a chip (MOV)

■ AUTHOR INFORMATION

Corresponding Author

Alireza Abbaspourrad − *Department of Food Science, College of Agriculture & Life Sciences, Cornell University, Ithaca, New York 14853, United States;* orcid.org/0000-0001-5617-9220; Email: Alireza@cornell.edu

Authors

Seyed Mohammad Davachi − *Department of Food Science, College of Agriculture & Life Sciences, Cornell University, Ithaca, New York 14853, United States;* orcid.org/0000-0001-7002-3708

Amir Mokhtare − *Department of Food Science, College of Agriculture & Life Sciences, Cornell University, Ithaca, New York 14853, United States*

Hooman Torabi − *Department of Food Science, College of Agriculture & Life Sciences, Cornell University, Ithaca, New York 14853, United States*

Mojtaba Enayati − *Department of Food Science, College of Agriculture & Life Sciences, Cornell University, Ithaca, New York 14853, United States;* Present Address: Center for

https://doi.org/10.1021/acsomega.2c07704
ACS Omega 2023, 8, 1710−1722

Materials and Manufacturing Sciences, Departments of Chemistry and Physics, Troy University, Troy, AL 36082, USA

Ted Deisenroth − *BASF Corporation, Tarrytown, New York 10591, United States*

Toan Van Pho − *BASF Corporation, Tarrytown, New York 10591, United States*

Liangliang Qu − *BASF Corporation, Tarrytown, New York 10591, United States*

Katrin-Stephanie Tücking − *BASF SE, Ludwigshafen am Rhein 67056, Germany*

Complete contact information is available at: https://pubs.acs.org/10.1021/acsomega.2c07704

Author Contributions

S.M.D: conceptualization, methodology, investigation, data curation, writing—original draft, writing—reviewing & editing. A.M.: conceptualization, investigation, data curation, writing—reviewing & editing. H.T.: investigation, data curation, writing—reviewing & editing. M.E.: investigation, data curation, writing—reviewing & editing. T.W.D.: conceptualization, resources, supervision, writing—reviewing & editing. T.V.P.: resources, supervision, writing—reviewing & editing. L.E.Q.: resources, supervision, writing—reviewing & editing. K.-S.T.: resources, supervision, writing—reviewing & editing. A.A.: conceptualization, supervision, project administration, funding acquisition, resources, writing—reviewing & editing.

Notes

The authors declare no competing financial interest.

■ ACKNOWLEDGMENTS

We would like to thank the Cornell Center for Materials Research (CCMR) for the use of their facilities. CCMR facilities are supported by the National Science Foundation (United States) under award number DMR-1719875. We would like to acknowledge the BASF Corporation for their continued support of academic and research pursuits.

■ REFERENCES

(1) Torabi, H.; Ramazani SaadatAbadi, A. R. Property Investigation of Poly (Ethylene Co-Vinyl Acetate)/Poly (l-Lactic Acid)/Organo Clay Nanocomposites. *J. Polym. Environ.* **2019**, *27*, 2886−2894.

(2) Perz, V.; Bleymaier, K.; Sinkel, C.; Kueper, U.; Bonnekessel, M.; Ribitsch, D.; Guebitz, G. M. Substrate Specificities of Cutinases on Aliphatic−Aromatic Polyesters and on Their Model Substrates. *New Biotechnol.* **2016**, *33*, 295−304.

(3) Wallace, P. W.; Haernvall, K.; Ribitsch, D.; Zitzenbacher, S.; Schittmayer, M.; Steinkellner, G.; Gruber, K.; Guebitz, G. M.; Birner-Gruenberger, R. PpEst Is a Novel PBAT Degrading Polyesterase Identified by Proteomic Screening of Pseudomonas Pseudoalcaligenes. *Appl. Microbiol. Biotechnol.* **2017**, *101*, 2291−2303.

(4) Kijchavengkul, T.; Auras, R.; Rubino, M.; Selke, S.; Ngouajio, M.; Fernandez, R. T. Biodegradation and Hydrolysis Rate of Aliphatic Aromatic Polyester. *Polym. Degrad. Stab.* **2010**, *95*, 2641−2647.

(5) Siegenthaler, K. O.; Künkel, A.; Skupin, G.; Yamamoto, M. Ecoflex and Ecovio: Biodegradable, Performance-Enabling Plastics. In *Synthetic Biodegradable Polymers*; Rieger, B., Künkel, A., Coates, G. W., Reichardt, R., Dinjus, E., Zevaco, T. A., Eds.; *Advances in Polymer Science*; Springer: Berlin, Heidelberg, 2012; pp 91−136.

(6) Weng, Y.-X.; Jin, Y.-J.; Meng, Q.-Y.; Wang, L.; Zhang, M.; Wang, Y.-Z. Biodegradation Behavior of Poly(Butylene Adipate-Co-Terephthalate) (PBAT), Poly(Lactic Acid) (PLA), and Their Blend under Soil Conditions. *Polym. Test.* **2013**, *32*, 918−926.

(7) Wang, H.; Wei, D.; Zheng, A.; Xiao, H. Soil Burial Biodegradation of Antimicrobial Biodegradable PBAT Films. *Polym. Degrad. Stab.* **2015**, *116*, 14−22.

(8) Woodard, L. N.; Grunlan, M. A. *Hydrolytic Degradation and Erosion of Polyester Biomaterials*; ACS Publications, 2018.

(9) Svoboda, P.; Dvorackova, M.; Svobodova, D. Influence of Biodegradation on Crystallization of Poly (Butylene Adipate-co-terephthalate). *Polym. Adv. Technol.* **2019**, *30*, 552−562.

(10) Künkel, A.; Becker, J.; Börger, L.; Hamprecht, J.; Koltzenburg, S.; Loos, R.; Schick, M. B.; Schlegel, K.; Sinkel, C.; Skupin, G.; Yamamoto, M. Polymers, Biodegradable. *Ullmann's Encyclopedia of Industrial Chemistry*; American Cancer Society, 2016; pp 1−29.

(11) Herzog, K.; Müller, R.-J.; Deckwer, W.-D. Mechanism and Kinetics of the Enzymatic Hydrolysis of Polyester Nanoparticles by Lipases. *Polym. Degrad. Stabil.* **2006**, *91*, 2486−2498.

(12) Chamas, A.; Moon, H.; Zheng, J.; Qiu, Y.; Tabassum, T.; Jang, J. H.; Abu-Omar, M.; Scott, S. L.; Suh, S. Degradation Rates of Plastics in the Environment. *ACS Sustainable Chem. Eng.* **2020**, *8*, 3494−3511.

(13) Saeedi Garakani, S.; Davachi, S. M.; Bagher, Z.; Heraji Esfahani, A.; Jenabi, N.; Atoufi, Z.; Khanmohammadi, M.; Abbaspourrad, A.; Rashedi, H.; Jalessi, M. Fabrication of Chitosan/Polyvinylpyrrolidone Hydrogel Scaffolds Containing PLGA Microparticles Loaded with Dexamethasone for Biomedical Applications. *Int. J. Biol. Macromol.* **2020**, *164*, 356−370.

(14) Tokiwa, Y.; Suzuki, T. Hydrolysis of Polyesters by Lipases. *Nature* **1977**, *270*, 76−78.

(15) Ribitsch, D.; Herrero Acero, E.; Przylucka, A.; Zitzenbacher, S.; Marold, A.; Gamerith, C.; Tscheließnig, R.; Jungbauer, A.; Rennhofer, H.; Lichtenegger, H. Enhanced Cutinase-Catalyzed Hydrolysis of Polyethylene Terephthalate by Covalent Fusion to Hydrophobins. *Appl. Environ. Microbiol.* **2015**, *81*, 3586−3592.

(16) Kleeberg, I.; Welzel, K.; VandenHeuvel, J.; Müller, R.-J.; Deckwer, W.-D. Characterization of a New Extracellular Hydrolase from Thermobifida Fusca Degrading Aliphatic− Aromatic Copolyesters. *Biomacromolecules* **2005**, *6*, 262−270.

(17) Ronkvist, Å. M.; Xie, W.; Lu, W.; Gross, R. A. Cutinase-Catalyzed Hydrolysis of Poly (Ethylene Terephthalate). *Macromolecules* **2009**, *42*, 5128−5138.

(18) Biundo, A.; Hromic, A.; Pavkov-Keller, T.; Gruber, K.; Quartinello, F.; Haernvall, K.; Perz, V.; Arrell, M. S.; Zinn, M.; Ribitsch, D. Characterization of a Poly (Butylene Adipate-Co-Terephthalate)-Hydrolyzing Lipase from Pelosinus Fermentans. *Appl. Microbiol. Biotechnol.* **2016**, *100*, 1753−1764.

(19) Tsutsumi, C.; Hayase, N.; Nakagawa, K.; Tanaka, S.; Miyahara, Y. The Enzymatic Degradation of Commercial Biodegradable Polymers by Some Lipases and Chemical Degradation of Them. *Macromolecular Symposia*; Wiley Online Library, 2003; Vol. *197*, pp 431−442.

(20) Baecker, M.; Schusser, S.; Leinhos, M.; Poghossian, A.; Schoening, M. J. Sensor System for the Monitoring of Degradation Processes of Biodegradable Biopolymers. *Sensors and Measuring Systems 2014*; ITG/GMA Symposium; VDE, 2014; Vol. *17*, pp 1−4.

(21) Schusser, S.; Krischer, M.; Bäcker, M.; Poghossian, A.; Wagner, P.; Schöning, M. J. Monitoring of the Enzymatically Catalyzed Degradation of Biodegradable Polymers by Means of Capacitive Field-Effect Sensors. *Anal. Chem.* **2015**, *87*, 6607−6613.

(22) Leinhos, M.; Schusser, S.; Bachmann, B.; Bäcker, M.; Poghossian, A.; Schöning, M. J. Micromachined Multi-parameter Sensor Chip for the Control of Polymer-degradation Medium. *Phys. Status Solidi A* **2014**, *211*, 1346−1351.

(23) Nghe, P.; Tabeling, P.; Ajdari, A. Flow-Induced Polymer Degradation Probed by a High Throughput Microfluidic Set-Up. *J. Non-Newtonian Fluid Mech.* **2010**, *165*, 313−322.

(24) Wouters, B.; Pirok, B. W.; Soulis, D.; Garmendia Perticarini, R. C. G.; Fokker, S.; van den Hurk, R. S.; Skolimowski, M.; Peters, R. A.; Schoenmakers, P. J. On-Line Microfluidic Immobilized-Enzyme Reactors: A New Tool for Characterizing Synthetic Polymers. *Anal. Chim. Acta* **2019**, *1053*, 62−69.

(25) Grayson, A. C. R.; Choi, I. S.; Tyler, B. M.; Wang, P. P.; Brem, H.; Cima, M. J.; Langer, R. Multi-Pulse Drug Delivery from a Resorbable Polymeric Microchip Device. *Nat. Mater.* **2003**, *2*, 767−772.
(26) Intra, J.; Glasgow, J. M.; Mai, H. Q.; Salem, A. K. Pulsatile Release of Biomolecules from Polydimethylsiloxane (PDMS) Chips with Hydrolytically Degradable Seals. *J. Controlled Release* **2008**, *127*, 280−287.
(27) Davachi, S. M.; Kaffashi, B. Preparation and Characterization of Poly L-Lactide/Triclosan Nanoparticles for Specific Antibacterial and Medical Applications. *Int. J. Polym. Mater. Polym. Biomater.* **2015**, *64*, 497−508.
(28) Kemala, T.; Budianto, E.; Soegiyono, B. Preparation and Characterization of Microspheres Based on Blend of Poly(Lactic Acid) and Poly(ε-Caprolactone) with Poly(Vinyl Alcohol) as Emulsifier. *Arab. J. Chem.* **2012**, *5*, 103−108.
(29) Das, P. P.; Huda, M. K.; Saikia, P. J.; Baruah, S. D. Study of the Formation of Biodegradable Polycaprolactone Particles Using Solvent Evaporation Method. *J. Macromol. Sci., Part A: Pure Appl.Chem.* **2019**, *56*, 69−75.
(30) Enayati, M.; Abbaspourrad, A. Cu(0)-Mediated Reversible-Deactivation Radical Polymerization of n-Butyl Acrylate in Suspension. *Polymer* **2018**, *153*, 464−473.
(31) Qin, D.; Xia, Y.; Whitesides, G. M. Soft Lithography for Micro- and Nanoscale Patterning. *Nat. Protoc.* **2010**, *5*, 491−502.
(32) Mokhtare, A.; Xie, P.; Abbaspourrad, A.; Rosenwaks, Z.; Palermo, G. Toward an ICSI Chip: Automated Microfluidic Oocyte Denudation Module. *Human Reproduction*; Oxford Univ Press Great Clarendon ST: Oxford OX2 6DP, England, 2020; Vol. *35*, pp 71−72.
(33) Weinberger, S.; Beyer, R.; Schüller, C.; Strauss, J.; Pellis, A.; Ribitsch, D.; Guebitz, G. M. High Throughput Screening for New Fungal Polyester Hydrolyzing Enzymes. *Front. Microbiol.* **2020**, *11*, 554.
(34) Herrero Acero, E.; Ribitsch, D.; Steinkellner, G.; Gruber, K.; Greimel, K.; Eiteljoerg, I.; Trotscha, E.; Wei, R.; Zimmermann, W.; Zinn, M.; Cavaco-Paulo, A.; Freddi, G.; Schwab, H.; Guebitz, G. Enzymatic Surface Hydrolysis of PET: Effect of Structural Diversity on Kinetic Properties of Cutinases from Thermobifida. *Macromolecules* **2011**, *44*, 4632−4640.
(35) Tong, H.; Jiang, Q.; Zhong, X.; Hu, X. Rhodamine B Dye Staining for Visualizing Microplastics in Laboratory-Based Studies. *Environ. Sci. Pollut. Res.* **2021**, *28*, 4209−4215.
(36) Ding, Y.; Lu, B.; Wang, P.; Wang, G.; Ji, J. PLA-PBAT-PLA Tri-Block Copolymers: Effective Compatibilizers for Promotion of the Mechanical and Rheological Properties of PLA/PBAT Blends. *Polym. Degrad. Stab.* **2018**, *147*, 41−48.
(37) Trubitsyn, G.; Nguyen, V. N.; Di Tommaso, C.; Borchard, G.; Gurny, R.; Möller, M. Impact of Covalently Nile Red and Covalently Rhodamine Labeled Fluorescent Polymer Micelles for the Improved Imaging of the Respective Drug Delivery System. *Eur. J. Pharm. Biopharm.* **2019**, *142*, 480−487.
(38) Baker, P. J.; Poultney, C.; Liu, Z.; Gross, R.; Montclare, J. K. Identification and Comparison of Cutinases for Synthetic Polyester Degradation. *Appl. Microbiol. Biotechnol.* **2012**, *93*, 229−240.
(39) Barth, M.; Oeser, T.; Wei, R.; Then, J.; Schmidt, J.; Zimmermann, W. Effect of Hydrolysis Products on the Enzymatic Degradation of Polyethylene Terephthalate Nanoparticles by a Polyester Hydrolase from Thermobifida Fusca. *Biochem. Eng. J.* **2015**, *93*, 222−228.
(40) Mueller, R.-J. Biological Degradation of Synthetic Polyesters—Enzymes as Potential Catalysts for Polyester Recycling. *Process Biochem.* **2006**, *41*, 2124−2128.
(41) Moreno-Villoslada, I.; Jofré, M.; Miranda, V.; Chandía, P.; González, R.; Hess, S.; Rivas, B. L.; Elvira, C.; San Román, J.; Shibue, T. π-Stacking of Rhodamine B onto Water-Soluble Polymers Containing Aromatic Groups. *Polymer* **2006**, *47*, 6496−6500.

https://doi.org/10.1021/acsomega.2c07704
ACS Omega 2023, 8, 1710−1722